



Improving air quality in high-density cities by understanding the relationship between air pollutant dispersion and urban morphologies



Chao Yuan^{a,*}, Edward Ng^a, Leslie K. Norford^b

^a School of Architecture, The Chinese University of Hong Kong, Shatin NT, Hong Kong

^b Department of Architecture, Massachusetts Institute of Technology, Cambridge, MA, United States

ARTICLE INFO

Article history:

Received 24 July 2013

Received in revised form

11 October 2013

Accepted 13 October 2013

Keywords:

Air pollution dispersion

CFD simulation

Building geometry

Urban permeability

High-density urban design

ABSTRACT

In high-density megacities, air pollution has a higher impact on public health than cities of lower population density. Apart from higher pollution emissions due to human activities in densely populated street canyons, stagnated air flow due to closely packed tall buildings means lower dispersion potential. The coupled result leads to frequent reports of high air pollution indexes at street-side stations in Hong Kong. High-density urban morphologies need to be carefully designed to lessen the ill effects of high density urban living. This study addresses the knowledge-gap between planning and design principles and air pollution dispersion potentials in high density cities. The air ventilation assessment for projects in high-density Hong Kong is advanced to include air pollutant dispersion issues. The methods in this study are CFD simulation and parametric study. The SST $k-\omega$ model is adopted after balancing the accuracy and computational cost in the comparative study. Urban-scale parametric studies are conducted to clarify the effects of urban permeability and building geometries on air pollution dispersion, for both the outdoor pedestrian environment and the indoor environment in the roadside buildings. Given the finite land resources in high-density cities and the numerous planning and design restrictions for development projects, the effectiveness of mitigation strategies is evaluated to optimize the benefits. A real urban case study is finally conducted to demonstrate that the suggested design principles from the parametric study are feasible in the practical high density urban design.

© 2013 Elsevier Ltd. All rights reserved.

1. Introduction

1.1. Background

People living in high-density cities suffer from both short and long term exposure to ambient air pollution. This causes severe health problems [1–3]. The risk of air pollution is relatively low to individual health but is considerably higher to public health [3]. Understanding the problem from the urban and city scale is therefore paramount.

Emissions from motor vehicles contribute to air pollution in urban areas, particularly at street canyon levels. The European Environment Agency (EEA) [2] has reported seven types of pollutants that people are exposed to, namely, particulate matter (PM), ozone (O₃), nitrogen dioxide (NO₂), sulfur dioxide (SO₂), carbon

monoxide (CO), heavy metals, as well as benzene (C₆H₆), and benzopyrene (BaP). All of these pollutants are primarily or secondarily related to road traffic (fossil fuel combustion). The World Health Organization (WHO) [1] has therefore explicitly recommended the concentration limits for various air pollutants such as O₃ and NO₂.

To decrease traffic pollution, an improved vehicle emission control program has been implemented in Hong Kong by the Hong Kong SAR Government. Nonetheless, the roadside concentration of NO₂ continues to increase [4]. Similar findings are also being reported in Europe by EEA [2]. High hourly, daily, and annual average concentrations of NO₂ have been recorded at the road-side stations in the Central, Causeway Bay, and Mong Kok areas in Hong Kong. Air pollution far exceeds the limits recommended by the WHO [4]. The three areas are high-density metropolitan areas and traffic hotspots. As shown in Fig. 1, vehicles crowd the streets of high-density urban areas in Hong Kong. The reported higher concentration of NO₂ is the result of the larger NO₂ percentage in total traffic emissions [2,5] and of poorer urban air ventilation in high-

* Corresponding author. Tel.: +852 67017286.

E-mail address: yach@cuhk.edu.hk (C. Yuan).



Fig. 1. Vehicle fleets in the deep street canyons of Mong Kok and Wan Chai in Hong Kong; high concentration of NO_2 is frequently measured at the roadside stations in the areas.

density urban areas [6,7]. The bulky building blocks, compacted urban volumes and very limited open spaces seriously block the pollutant dispersion in these deep street canyons [8,9]. Therefore, apart from having control measures to decrease vehicle emissions, understanding pollutant dispersion as related to the urban planning and design mechanism is necessary in order to guide policy-makers, planners, and architects in making better evidence-based decisions.

1.2. Literature review

Several studies on urban climate in the past decades have focused on air quality in the street canyons [10]. In some studies, the “car-chasing” experiment and tunnel testing have been conducted [11,12] to determine the real-world traffic emission factors of particles and gaseous pollutants, and to evaluate the chemical compositions of emissions from different vehicles. These studies provided important information for evaluating the effects of different pollutants on public health, and to assist in drawing up guidelines for policymakers to implement transportation control measures. These studies are also important references as the input boundary conditions for pollutant dispersion modeling.

Computational fluid dynamics (CFD) studies in different scales have been conducted by researchers to identify the dispersion phenomenon in street canyons. Pollutant dispersion has been investigated in idealized street canyons with a point or line emission source with [13,14] or without chemical reaction [9,15–18]. Researches on isothermal and non-isothermal street canyons, in which the effects of convective and turbulent mass fluxes on dispersion were studied, have been reported [19,20]. These studies have provided important information on pollutant dispersion patterns, as well as on the relationship among wind velocities, turbulence intensities, and pollutant dispersion. By cross-comparing the modeling results with wind tunnel experiment data, these studies have also evaluated the performances of their dispersion and turbulence models.

Urban microclimate and air quality can be seen both as the consequence and as the prerequisite of urban planning and design activities. Therefore, the reciprocal relationship between them requires research on the environmental sensitivity of urban planning and design, in order to positively address their negative consequences on urban air quality. Mirzaei and Haghighat [21] provided a systematic approach to quantify the outside environment in the street canyon. Huang et al. [20] studied an actual urban case of mid-density layouts. Hang et al. [8] conducted a study on the effects of varying building heights on street level air pollutant dispersion and

Eefents et al. [22] reported the effects of canyon indicators such as Sky View Factor (SVF) on the concentration of NO and NO_x . Buccolieri et al. [23] clarified the influence of the building packing density on the pollutant concentration. Richmond-Bryant [24] related the fluid properties and canyon geometries, such as the Reynolds number and canyon height, with air pollutant retention by field measurement data at Manhattan and Oklahoma. However, the direct understandings for design strategies behind a decrease in pollutant concentration through urban morphological mechanisms, particularly for high-density cities, remains little known. Further parametric studies are needed to extend the study findings for practical design applications. Bridging the knowledge gap between high-density urban design and air pollutant dispersion mechanisms in the urban street canyons is necessary to provide guidance for planners, designers and policymakers.

1.3. Objectives

The Severe Acute Respiratory Syndrome (SARS) episode in 2003 triggered the Air Ventilation Assessment (AVA) study in Hong Kong. Since 2006, AVA has been implemented as a prerequisite for urban development and old-district redevelopment [25]. Major government projects have been required to conduct an AVA by following the Technical Circular No. 1/06 guideline. Furthermore, the “Sustainable Building Design (SBD) Guidelines (APP-152)” have also been drawn up by the Hong Kong Government. These allow architects to evaluate the effects of their proposed buildings on the surrounding wind environments, and to enhance urban environmental design by prescriptively applying three user-friendly strategies: building setback, building separation, and greenery [26].

This study builds on the previous work [27] by conducting parametric studies to statistically evaluate and further develop the efficacy of the AVA TC-1/06 guidelines and the SBD’s APP-152 guidelines with regard to air pollutant dispersion. The study aims to provide important and sufficiently accurate insights at the beginning stage of the design practice. These insights are helpful to avoid the mistakes that cannot be easily corrected at the late stages of the design practice. The results of this study are intended to facilitate a paradigm shift from the typical experience-based ways of designing and planning to a more scientific, evidence-based process of decision making, which is necessary to cope with the needs of designing high density cities [28].

This study firstly evaluates the performance of both the Reynolds-averaged Navier–Stokes (RANS) and Large Eddy Simulation (LES) models in modeling species transport through a validation study so as to identify the optimal modeling method for the parametric study.

Secondly, a series of parametric studies is conducted to understand the relationship among building geometry, urban permeability, and air pollutant dispersion. These studies evaluate the effects of future urban developments, based on the current planning trend, on air pollutant dispersion in the street canyons. The knowledge of the efficacy of various mitigation strategies for better air quality at urban areas is provided. Given the finite land resources in high-density cities and the numerous planning and design restrictions for development projects, the evaluation of the effectiveness of mitigation strategies is needed to optimize the benefits. To avoid reducing the land use efficiency, the plot ratio in all of the cross-comparison scenarios are same.

2. Modeling method

The modeling method of this study is CFD simulation. This has already been used not only as an environmental research tool, but also as a design tool for urban planners and designers [29]. ANSYS Fluent CFD Software Package (version 14.0) was used for this study.

2.1. Eulerian method for species transport modeling

This study used the Eulerian method to investigate the efficiency of different design strategies on air pollutant dispersion. The Eulerian and the Lagrangian methods are widely used to model air pollutant dispersion [15,30,31]. Compared with the Lagrangian method, which considers the species as a discrete phase, the Eulerian method considers species as a continuous phase and is solved based on a control volume, which is similar in form to that for the fluid phase [30,31]. Therefore, the Eulerian method is more convenient for calculating the air pollutant concentration, which was the index this study used to evaluate air pollutant dispersion. Another reason for choosing the Eulerian method was that it has lower computational demands than the Lagrangian method, which needs to track more than several million particles in the large computational domain for outdoor environment simulation. The Eulerian method has been validated by researchers comparing the simulated data with wind tunnel experiment results [15,30].

In this study, ANSYS Fluent was used to solve the unsteady convection-diffusion equation to predict the mass fraction of species Y_i [32]:

$$\frac{\partial}{\partial t}(\rho Y_i) + \nabla \cdot (\rho \vec{v} Y_i) = -\nabla \cdot \vec{J}_i + S_i + R_i \quad (1)$$

Where S_i is the rate of the user-defined source term, i is the number of species, ρ is the air density, \vec{v} is the overall velocity vector, t is time, and \vec{J}_i is the mass diffusion in turbulent flows. Inlet diffusion is enabled to include the diffusion flux of species at the emission inlet. Because the simulation excludes chemical reaction, the rate of the product from chemical reaction (R_i) is set to zero. \vec{J}_i in the turbulence is estimated as [32]:

$$\vec{J}_i = -\left(\rho D_{i,m} + \frac{\mu_t}{Sc_t}\right) \nabla Y_i - D_{T,i} \frac{\nabla T}{T} \quad (2)$$

Where $D_{i,m}$ and $D_{T,i}$ are the mass diffusion coefficient for species i and the thermal diffusion coefficient, respectively, Sc_t is the turbulent Schmidt number (the default value 0.7 is used in this study), and μ_t is the turbulent viscosity.

2.2. Optional turbulence model: a validation study

The wind tunnel data provided by Niigata Institute of Technology [16] was used to validate the above mentioned air pollutant

dispersion modeling method. The effects of the different turbulence models on air pollutant dispersion were also investigated in this validation study, in which the standard and realizable $\kappa-\epsilon$ model, Reynolds stress model (RSM), shear-stress transport (SST) $\kappa-\omega$ model, and LES were included.

The model configurations were set to match those in the wind tunnel experiment, as shown in Fig. 2. The H/W and H/L aspect ratios were set to 1.0 and 0.5, respectively, where H is the building height, W is the width of the street, and L is the length of the canopy. All modeling settings followed the Architectural Institute of Japan (AIJ) guideline [33], such as domain size ($X \times Y \times Z$: 600 m \times 200 m \times 100 m), grid type (structural grid), grid resolution (grid number: 3 million, and the grid size at street canyon was set at less than 1/10 of building length), grid size ratio (maximum grid size ratio was set at 1.3). More than three grid layers were used under the test line, and the convergence criteria for turbulence and species were E-05 in the RANS model and E-04 in the LES modeling. The input wind direction was perpendicular to the street canyon. Input wind velocity (U_x) and turbulence kinetic energy (TKE) profiles plotted in Fig. 2 were set by a user-defined function. The surface roughness factor (α) was set at 0.21. The modeling settings were summarized at Table 1.

The calculation is steady in the RANS study and is unsteady in the LES study. The time step in LES was set constant, $\Delta t = 0.001$ s, and the solution variables were time-averaged until the flow became statistically steady, which was identified by monitoring the instantaneous values of variables at several points in the street canyon. The sampling time (t) was approximately 180 s. The Smagorinsky–Lilly model provided by ANSYS Fluent 14.0, where $C_s = 0.12$ as recommended by Tominaga and Mochida [34], was used in the LES modeling.

As shown in Fig. 2, the point source was arranged at the middle of the street canyon. Ethylene (C_2H_4) was used as the tracer gas and was released from the point source in the model with a wind velocity W_s ($W_s/U_b = 0.12$, U_b was the input wind velocity at the building height, 3.8 m/s). The tracer concentration was set at 1000 ppm, duplicating the setting in the wind tunnel experiment.

The simulation results of the different turbulent models were collected at three test lines in Fig. 2 and cross-compared in Fig. 3. As reported by Tominaga [16], because of the reproduction of the instantaneous fluctuation of the concentration, the emission concentration can be more accurately modeled by a LES model than by a RANS model, particularly at the windward area in the street canyon. However, the computational cost of the LES model is several times higher than that of the RANS model.

On the other hand, the performance of the RANS models provided by ANSYS Fluent 14.0 was significantly better than the ones reported by Tominaga [16]. The simulation results were closer to the experiment data particularly at the bottom line ($X/H = 0.1$, X is the height of the test line). However, all RANS models overestimated the concentrations at the middle and top lines ($X/H = 0.5$ and 1, respectively), particularly at the windward side of the street canyon. Among the models, the SST $\kappa-\omega$ model (the red dash line) performed best in terms of air pollutant modeling at the windward side. The special near-wall region (the shear layer) treatment by the standard $\kappa-\omega$ model [32,35] was considered helpful for estimating the air pollutant concentration near surface regions. Balancing the computational cost and accuracy, for this study, the SST $\kappa-\omega$ model was selected as the preferred turbulence model to simulate the air pollutant dispersion of the cases in the parametric study. Furthermore, the SST $\kappa-\omega$ model was considered to be a good tool for modeling air pollutant dispersion in the design process, for which it offers acceptable accuracy and computational cost.

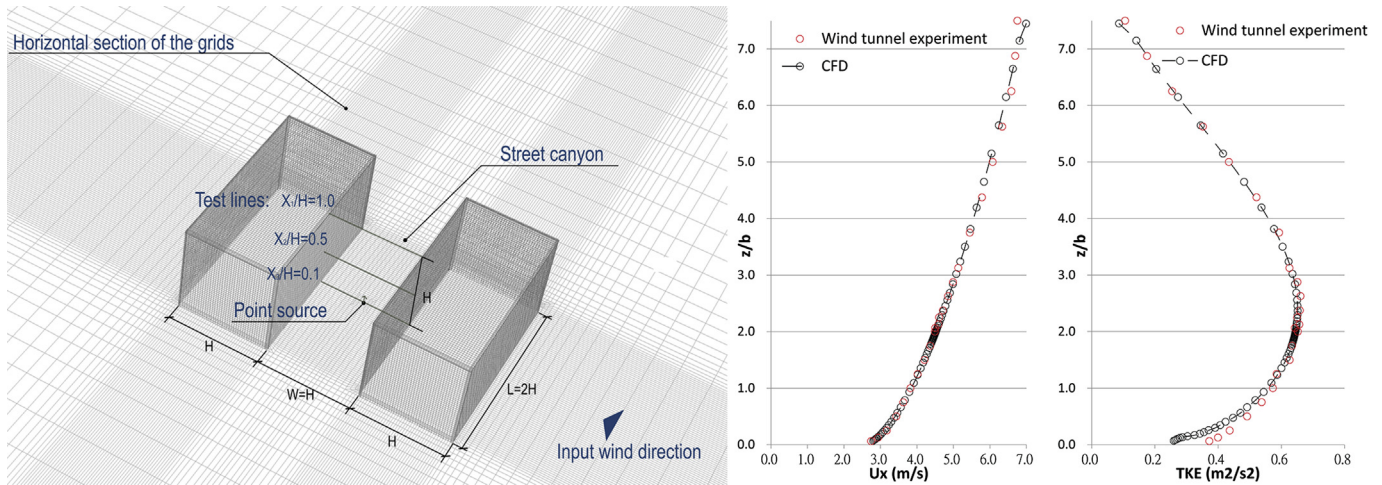


Fig. 2. Model configurations, Input conditions (U_x and TKE), and horizontal test lines in the street canyon; X_1 , X_2 , and X_3 are the heights of the test lines.

3. Methodology

3.1. Parametric study

Compared with other methods used in studies that focused on real urban morphologies [36–38], obtaining generic information for deriving guidelines is easier by using parametric studies. By cross-comparing the sensitivity of species dispersion to the parameter changes in various testing scenarios, the critical design elements can be efficiently identified. For example, the results of the parametric study of the wing wall for room ventilation by Givoni [39] were implemented by the Hong Kong government [40]. For results of parametric studies to be relevant, scenarios should resemble the reality [40]. An urban-scale model is therefore used in this study to obtain realistic parametric simulation results. As shown in Fig. 4, the parametric geometric models were established based on the actual urban conditions in Mong Kok (a high density downtown area in Hong Kong) using a regular street grid. This model should realistically resemble air

flows and air pollutant dispersion status in the actual street canyons. Unlike several earlier parametric studies in which only one or two generic buildings or building arrays were included [7,9,15–17,41,42], the effects of the urban context were included in this study.

As shown in Fig. 5, eight geometric cases were designed to create their corresponding parametric models, establishing a total of eight simulations with different building geometries and urban permeability. Their details were tabulated in Table 2. Cases 1 and 2 represented the current and future urban conditions respectively. Cases 3 to 8 were established based on the sustainable building design (SBD-APP-152) guidelines [26]. In Cases 3 to 5, three design strategies – building setback (Strategy A), building separation (Strategy B), and stepped podium void (Strategy C) – were implemented respectively. Building porosities were included in Case 6 (Special Strategy). For Cases 7, building setback was combined with building separation. For Case 8, stepped podium void was combined with building separation.

Plot ratios of Cases 3 to 8 were set to be same to that of Case 2. This normalized their development potential. For example, the loss of floor area caused by incorporating mitigation strategies was compensated by increasing the building height in Cases 3 to 8.

Given the different building geometries, the corresponding urban permeability of the eight cases were different, as shown in Table 2. The permeability of buildings (P) [26] and site area ratio (λ_p), which respectively represent the vertical and horizontal permeability, were calculated. High values of P and λ_p indicate low permeability.

3.2. Modeling settings in the parametric study

A total of eight testing scenarios were simulated by both the Eulerian species transportation model and the SST $\kappa-\omega$ turbulence model to evaluate the species dispersion in street canyons. As shown in Fig. 6, the computational domain size was $3.9 \text{ km} \times 4 \text{ km} \times 0.55 \text{ km}$ ($X \times Y \times Z$). Other simulation settings were similar with the validation study in Section 2.2.

To set the input wind velocity profile particularly for the Mong Kok area by means of the log law, the site-specific annual wind data ($U_{\text{met}} = 11 \text{ m/s}$) at a 450 m height (d_{met}) were obtained from the fifth-generation NCAR/PSU meso-scale model (MM5) [43] and, given the high urban density of Hong Kong, the surface roughness factor (α) was set at 0.35.

Table 1
Simulation modeling settings.

Computational domain	$X \times Y \times Z$: $600 \text{ m} \times 200 \text{ m} \times 100 \text{ m}$
Blockage ratio	<5%
Grid expansion ratio	Less than 1.3
Grid resolution	Grid size less than 1/10 of building length at the street canyon (Fig. 2) Grid number: 3 million
Grid type	Structural grid (Fig. 2)
Prismatic layer	More than three grid layers under the test line
Inflow boundary condition	Input wind velocity (U_x) and turbulence kinetic energy (TKE) profiles reproduced by a user-defined function, based on the measurement at the wind tunnel experiment (Fig. 2)
Outflow boundary condition	Zero gradient condition
Near wall treatment	Enhanced wall functions in $\kappa-\epsilon$ models and Reynolds stress model No wall functions in SST $\kappa-\omega$ and LES model
Solving algorithms	QUICK for momentum, TKE, and other convection terms
Relaxation factors	Default values in ANSYS Fluent 14.0
Convergence criteria	Below E-05 in RANS model Below E-04 in LES model

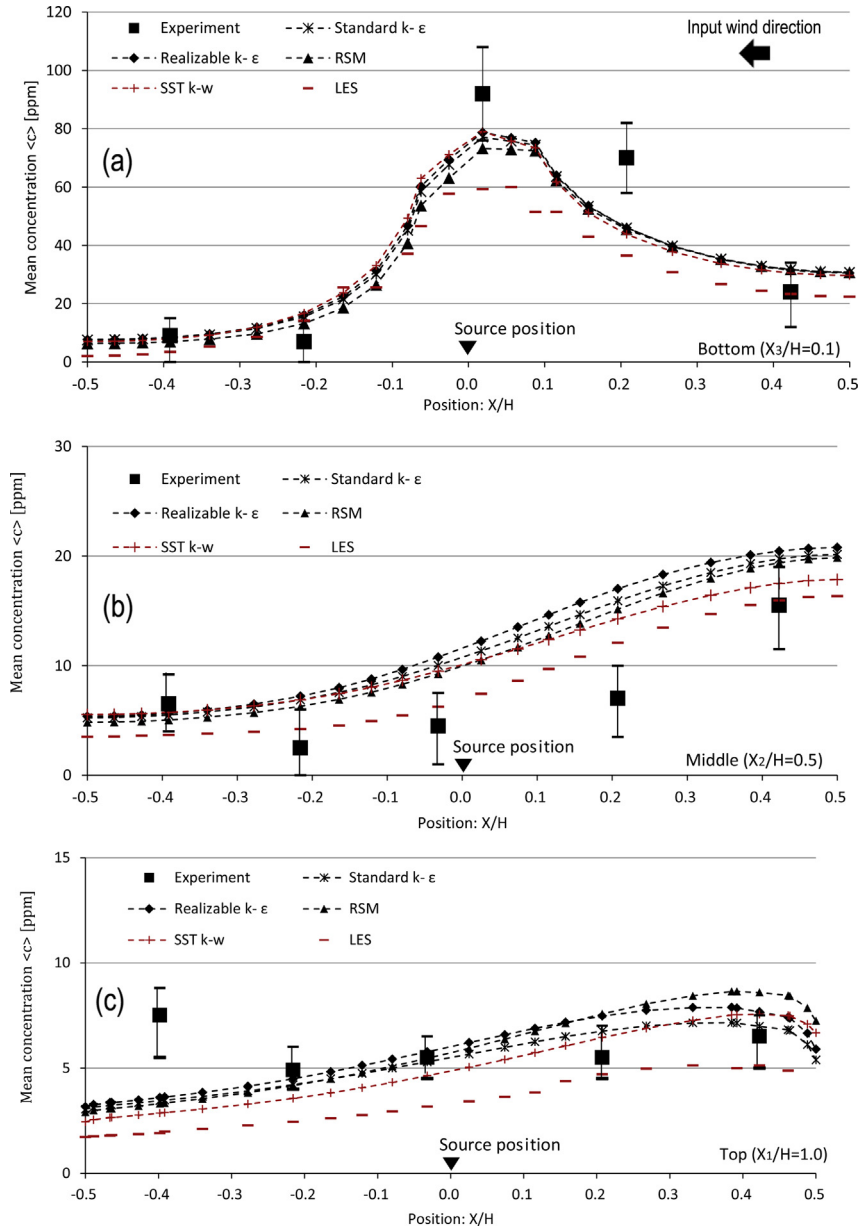


Fig. 3. Cross-comparisons of time-averaged concentrations $\langle c \rangle$ at the street canyon between the wind tunnel experiment and different turbulent models: a) $\langle c \rangle$ at the bottom line ($X_3/H = 0.1$); b) $\langle c \rangle$ at the middle line ($X_2/H = 0.5$); c) $\langle c \rangle$ at the top line ($X_1/H = 1.0$). Error bars are the standard deviations of the measurements in the wind tunnel experiments.

NO_2 was selected as the emission gas as its concentration is still increasing in the metropolitan areas in Hong Kong. A line pollutant source ($X \times Y$: 1300 m \times 10 m) was set at the bottom of the street canyon in the middle of a building gap to represent the major road with heavy traffic volume at Mong Kok, as shown in Fig. 6. A reference emission NO_2 concentration ($\langle c_0 \rangle = 1000$ ppm) was used. The input wind velocity ratio at the emission source followed the value used in the wind tunnel experiment [16], $W_s/U_b = 0.12$.

Chemical reactions between NO_x and ozone (O_3) [44] were not factored in this study as it aimed to determine how NO_2 could be dispersed and transported by air flow in street canyons with different geometric parameters. The study was therefore limited to the city spatial scale, which is the space of the street canyons.

4. Result analysis and discussion

This study used the normalized concentration (\bar{c}) as the index to analyze the effects of different urban permeability and building geometries on air pollutant dispersion in the street canyon. This was given by:

$$\bar{c} = \langle c \rangle / \langle c_0 \rangle \tag{3}$$

Where $\langle c \rangle$ is the modeling result of the time-averaged concentration of NO_2 and $\langle c_0 \rangle$ is the reference emission concentration, the norm of $\langle c \rangle$. Given the definition of \bar{c} , the threshold value of \bar{c} was set to 1.0. When the value of \bar{c} is less than 1.0, air pollutants start to disperse and do not concentrate in the street canyon.

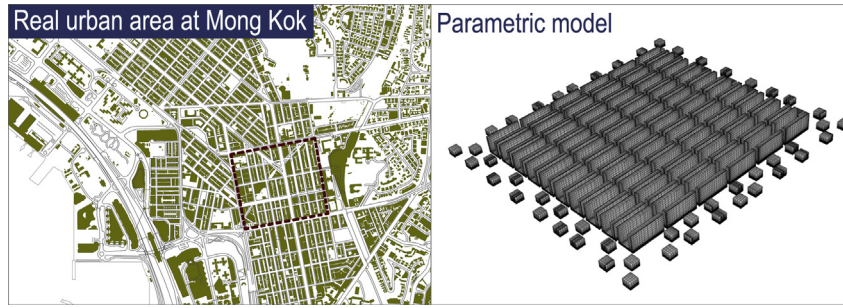


Fig. 4. Real urban area located at Mong Kok and its corresponding parametric model.

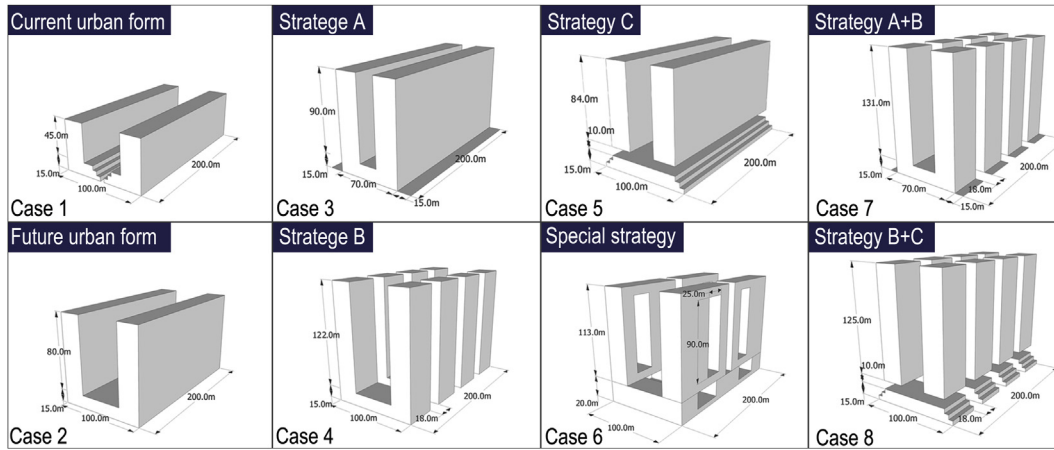


Fig. 5. Eight testing scenarios.

In addition to the analysis of contours of the normalized concentration, statistical studies were also conducted to evaluate the implied importance of design strategies for high-density urban areas, and to cast further light, if any, on the sustainable building design guidelines [26]. Furthermore, the discussion section was provided to further clarify the reasons of the observed dispersion phenomenon in scenarios with different urban permeability and building geometries.

4.1. Cross-comparison based on normalized concentration contours

The contours of the normalized concentration on the horizontal planes (2 m above the ground) and vertical planes of the eight cases were respectively shown in Figs. 7 and 8. This was to give an intuitive grasp of the sensitivity of air pollutant dispersion with respect to the changes in building geometries and urban permeability.

As shown in Fig. 7a, it was evident that the values of \bar{c} in street canyons with emission sources were high in Case 1, the current case. Most values of pedestrian-level normalized concentration in streets with emission sources were larger than the threshold value (1.0), indicating that air pollutant was not dispersed but was concentrated at the pedestrian height levels. The vertical distributions shown in Fig. 8 indicated that the condition may worsen in the future, Case 2. The values of \bar{c} in Case 2 were larger than 1.5 at the entire podium layer (0 m–15 m).

On the other hand, mitigation strategies in Cases 3 to 8 can, in various degrees, lead to better air pollutant dispersion, as shown in Fig. 7b and c. On the whole, even though Cases 3 to 8 had higher plot ratios than Case 1, and had the same plot ratio as Case 2 (Table 2), they had less stagnant areas. It should be noticed that the dispersion paths were significantly different. In Cases 4 to 8, most of the emitted air pollutant was diluted by the horizontal airflows through the permeable building as shown in Fig. 8. Thus, only a

Table 2
Eight testing scenarios in which air flows and species transportation were simulated.

Testing scenario	Case	Building geometry		Land use efficiency		Urban permeability		
		Parameter	Strategy style	H (m)	Plot ratio	P	λ_p	λ_i
1	Case 1	Current urban form	/	60	8.9	0.9	0.7	0.9
2	Case 2	Future urban form	/	95	14	0.9	0.8	0.9
3	Case 3	Building setback	Single	105	14	0.9	0.5	0.7
4	Case 4	Building separation	Single	137	14	0.7	0.6	0.5
5	Case 5	Stepped podium void	Single	109	14	0.8	0.6	0.7
6	Case 6	Building porosity	Single	133	14	0.7	0.8	0.7
7	Case 7	Building separation + Building setback	Multiple	146	14	0.7	0.4	0.3
8	Case 8	Building separation + stepped Podium void	Multiple	150	14	0.6	0.4	0.4

Note: H: Building height; P: Permeability of buildings ($P = \text{Sum of projected building areas/area of the assessment zone}$ [26]); λ_p : Site coverage ratio [45]; λ_i : Integrated permeability (the calculation method was provided in Section).

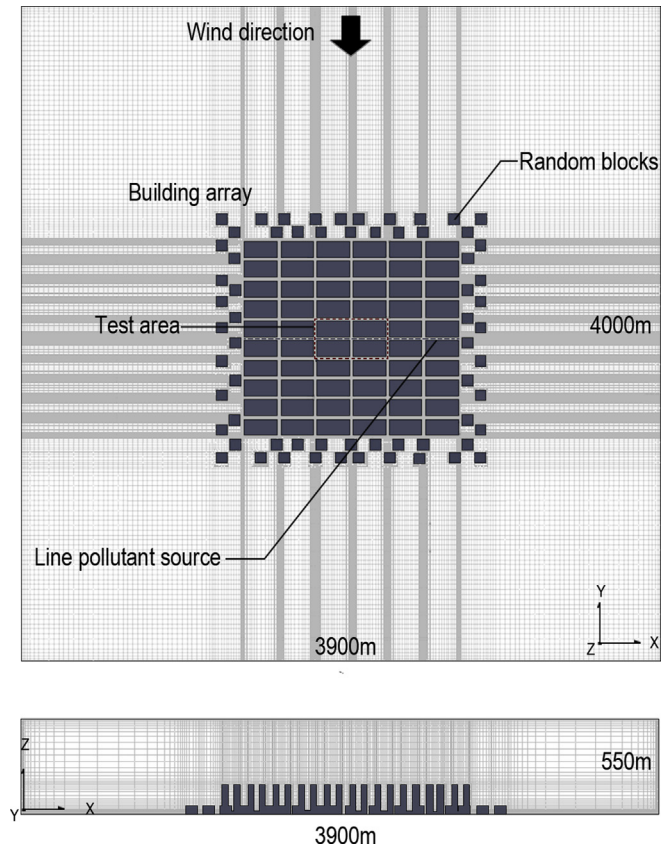


Fig. 6. Modeling configurations in the parametric study. The surrounding random blocks represent the surrounding urban surface roughness.

small amount was diffused away from the top of canyon. By contrast, the air pollutant was mainly diffused from the top of canyon in Case 3.

4.2. Statistically weighted cross-comparison

A statistical analysis was conducted for the evaluation of the importance of various design strategies on the air pollutant dispersion. The data collected at the horizontal test line of the pedestrian area was for the outdoor air pollutant concentration evaluation. The data collected at the vertical test line in the center of the building gap was to evaluate the effect of building geometries on the indoor air quality in the roadside buildings, because the vertical distribution of the normalized concentration. It is evident that the differences among cases were larger than the reported uncertainty shown in the validation study results, meaning that the differences are significant.

As shown in Fig. 9, the data of the normalized concentrations (2 m above the ground) collected at the horizontal line at the pedestrian area were plotted together. In Fig. 9a, the normalized concentration in Case 1 were plotted using a red solid line as a baseline case to cross compare the cases with single mitigation strategies (Cases 3–6). The threshold value of the normalized concentration was also highlighted. Case 3 can disperse the air pollutant at the streets parallel with the input wind direction, but cannot disperse the air pollutants in the target street canyon, only decreasing \bar{c} about 0.1–0.2. The performances of Cases 4 to 6 were significantly better than that of Case 3. Most values of \bar{c} were less than 1.0 in Case 4. The stepped podium void in Case 5 did not promote air pollutant dispersion as much as in Case 4. Most values

of \bar{c} in Case 5 were slightly above the threshold value. But an approximately 0.4 decrease of \bar{c} was still observed. The performance of Case 6 was better than Case 5 and similar to Case 4, as most values of \bar{c} were less than 1.0.

The multiple design strategies in Cases 7 and 8 were compared with Case 4 in Fig. 9b to clarify the efficiency of combining single strategies. The performance of Case 7 was similar to Case 8, and fractionally better than Case 4 (about 0.1 of \bar{c} values). The values of \bar{c} for the entire street were less than 1.0 in both Case 7 and 8.

The vertical distributions of the normalized concentration at the center of the building gap (vertical test line) were plotted in Fig. 10. Results indicated that the values of \bar{c} were larger than 1.0 below 30 m and 60 m respectively in Cases 1 and 2. It indicated that a deterioration in indoor air quality could occur in the roadside buildings at both height ranges due to outside traffic air pollutants, particularly for the residential building in which natural ventilation is typically adopted.

As shown in Fig. 10, the building setback in Case 3 did not mitigate this negative impact effectively. However the other design strategies successfully decreased pollutant concentrations. High concentration was only observed at 0 m–10 m height. With these design strategies, roadside buildings can enjoy natural ventilation and will not suffer from outside traffic air pollutants. This result is particularly important for urban design with residential land use.

4.3. Discussion of the cross-comparison results

The above analysis clarified that, in general, the effects of building geometry on pollutant dispersion in street canyons are similar to the effects on pedestrian-level natural ventilation (which underlie the AVA guidelines). However, a significant difference should be emphasized: air pollutant dispersion significantly depends on the permeability of the entire street canyon layer. Interestingly, the incorporation of building porosity in Case 6, which had previously been shown as a poor mitigation strategy for improving the performance of pedestrian-level air ventilation [27], can effectively improve air pollutant dispersion both horizontally and vertically.

To further describe air pollutant dispersion in the street canyon and explain the cross-comparison results, the vertical distribution of the normalized concentration (\bar{c}), turbulent intensity (I), and wind speed (U) at the vertical test line in the center of the building gap were plotted in Fig. 11.

The analysis indicated that turbulent diffusion played a major role in pollutant dispersion in cases with low permeability (Cases 1–3: $P = 0.9$), and the pollutant dispersion significantly depends on convection effects in high permeability cases (Cases 4 to 6: $P = 0.7–0.8$). In Cases 1 to 3, the value of \bar{c} in the street canyon displayed almost constant decreases with height. Regression analysis indicated that the vertical distribution of \bar{c} in the low permeability cases (Case 1–3) significantly depended on the turbulent intensity (I) ($R^2 = 0.87$), but no relationship between the normalized concentration and turbulent intensity ($R^2 = 0.11$) was observed in high permeability cases (Case 4–6), as shown in Fig. 12.

In cases with higher permeability, building separation, stepped podium void, and building porosity all increased the effect of convection on pollutant dispersion. The normalized concentration did not depend on turbulent intensity, as shown in Fig. 12, and did not constantly decrease with height. As shown in Fig. 11, the normalized concentration rapidly decreased until the height of building permeability and then slowly developed to an asymptotic value. In Cases 5 and 6, even though wind speed and turbulence intensity largely decreased above the height of the building permeability, the normalized concentration remained at a low level because the building permeability let clean air flow horizontally into the street

canyon, diluting and transporting air pollutant out of the street canyon. The building permeability in Case 4 was achieved by building separations that range from the ground level to the top of the building. Therefore, the strategy in Case 4 was better than in other cases. The building porosity in Case 6 provided more building permeability than Case 5, so that the pollutant dispersion in Case 6 was better than Case 5.

Based on the above analysis, it was considered that, to lower air pollutant concentrations, strategies to promote convection effects, such as building porosity, separation and podium void, may be more efficient than the strategies for larger turbulent diffusion such as building setback. This finding is also explained the cross-comparison results in Sections 4.1 and 4.2.

Furthermore, further examining the eight contours of the normalized concentration on the pedestrian level Fig. 7 indicated that, in high-density cities, the direction of dispersion of pedestrian-level air pollutants depends on both input wind direction and the urban permeability. In Cases 1–3 ($P = 0.9$) with low

permeability, pedestrian-level air flow was reversed, contrary to the input wind direction, so that air pollutant were transported upwind of the pollutant source. In contrast, in Cases 4–8 with high urban permeability ($0.6 \leq P \leq 0.8$), air pollutants were mainly dispersed downwind of the pollutant source. Therefore, unlike the understandings for low density cities, it is not dependable to estimate the direction of pollutant dispersion at the pedestrian-level in high-density cities solely based on the prevailing wind direction. For a reliable estimation, the urban permeability also needed to be taken into consideration.

4.4. Effects of urban permeability

This study also conducted a linear regression analysis to statistically weight the effects of P and λ_p on the spatially averaged pollutant concentration. The results were plotted together in Fig. 13. It was clear that the spatially-averaged normalized concentration depends on the permeability of buildings (P) more than

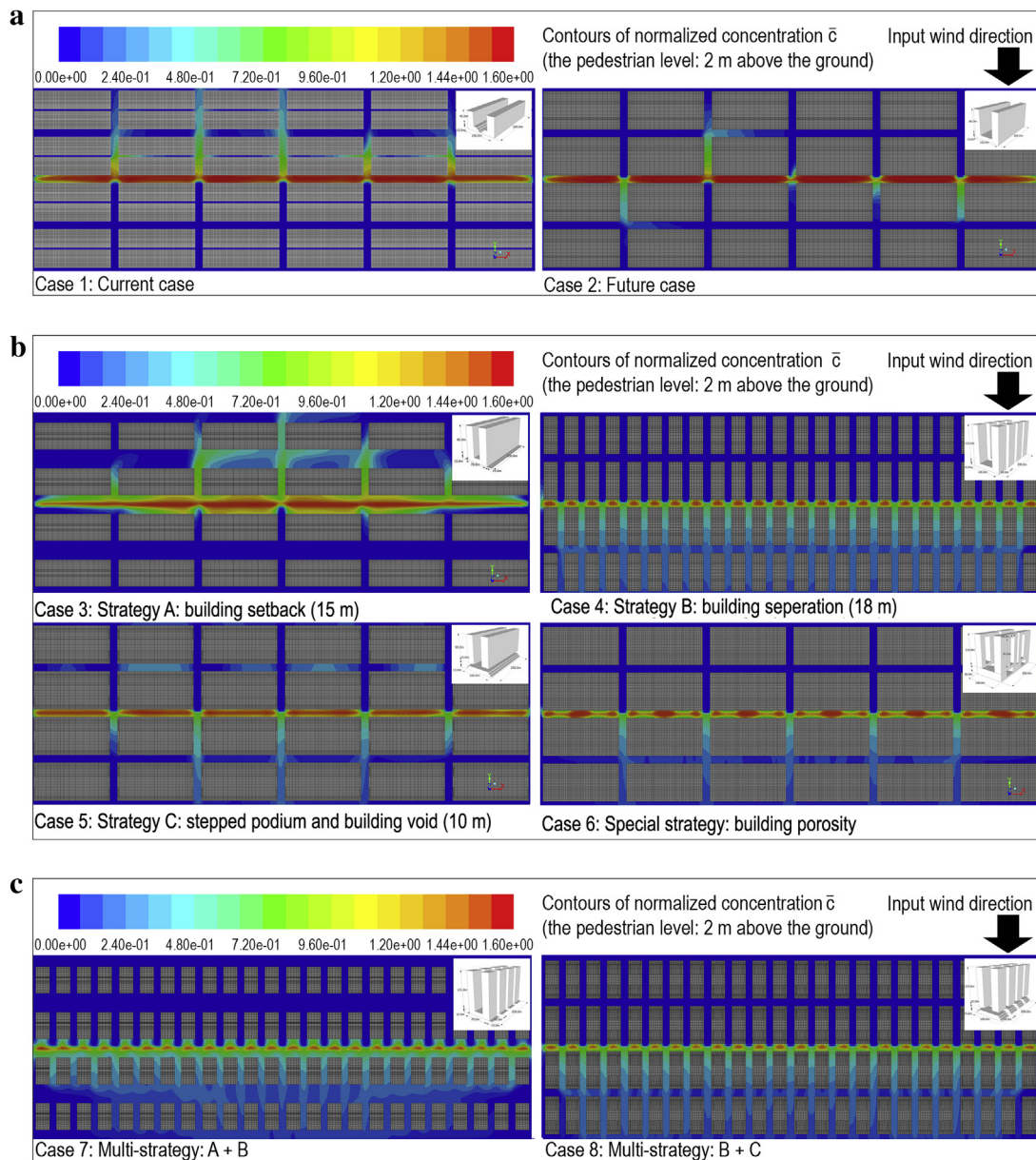


Fig. 7. a): Contours of \bar{c} at the pedestrian level (2 m above the ground) in Cases 1 and 2. (b): Contours of \bar{c} at the pedestrian level (2 m above the ground) in Cases 3–6 with single mitigation strategies. (c): Contours of \bar{c} at the pedestrian level (2 m above the ground) in Cases 7 and 8 with multi mitigation strategies.

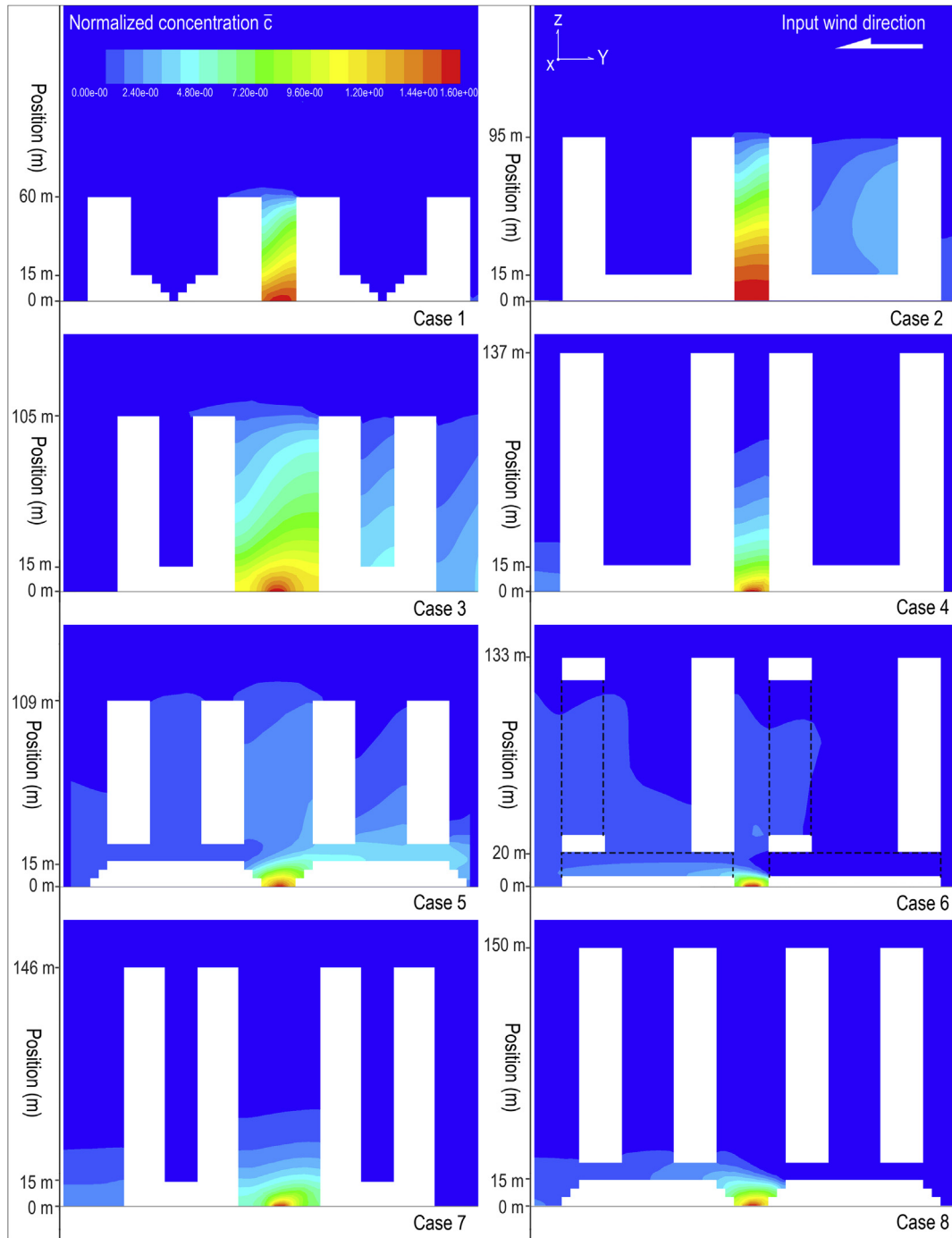


Fig. 8. Contours of \bar{c} at the vertical planes in total eight cases.

on the site coverage ratio (λ_p), as R^2 for P is 0.78 larger than R^2 (0.47) for λ_p .

Furthermore, to better predict spatially-averaged \bar{c} in urban areas, the integrated permeability λ_i was calculated based on Counihan’s roughness model [45] for estimating urban permeability as follows:

$$\lambda_i = P \cdot (C_1 \lambda_p + C_2) \tag{4}$$

The coefficients C_1 (1.4352) and C_2 (0.0463) [45] were for the contribution of λ_p , considering that λ_p , as the horizontal permeability, is less important than P, as the vertical permeability. The values of λ_i in all eight cases were given in Table 2.

As shown in Fig. 13, a strong relationship between λ_i and spatially averaged \bar{c} ($R^2 = 0.83$) indicated that λ_i is a good urban permeability index to estimate traffic air pollutant dispersion. This understanding provided a possibility for mapping traffic air pollutant concentrations in urban areas with traffic volume data by using GIS technology.

5. Urban implementation based on the real case study

A real case study at Mong Kok was conducted to demonstrate that the suggested design principles and understandings were

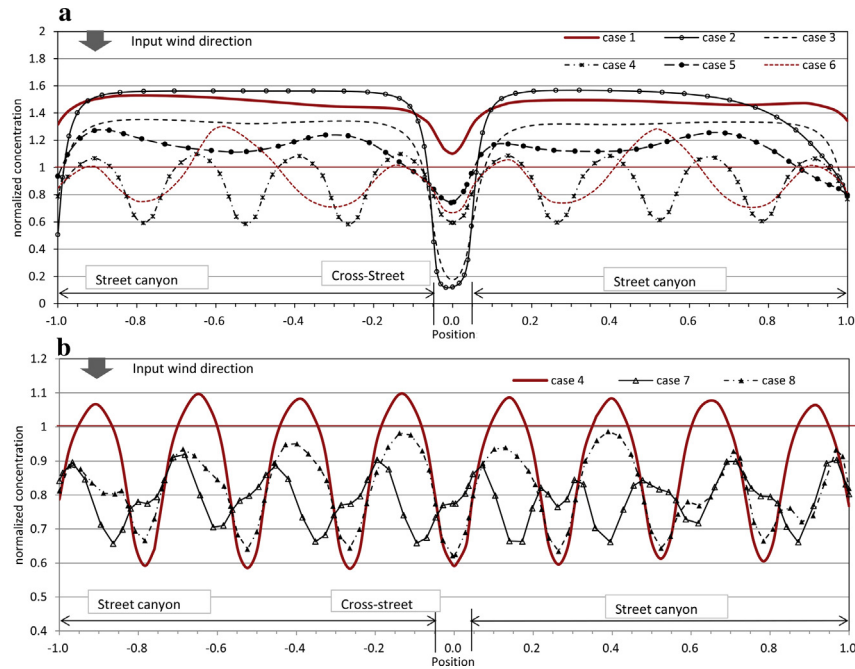


Fig. 9. (a): Cross comparison of the horizontal distributions of normalized concentration (\bar{c}) in Cases 1–6. (b): Cross comparison of the horizontal distributions of the normalized concentration (\bar{c}) in Cases 4, 7, and 8.

feasible in real urban design practice. As shown in Fig. 14, based on the current urban morphology (Case 1), an urban design (Case 2) was produced to improve the air quality at this high-density urban area. Based on the characteristic of different buildings, different mitigation design strategies were employed in every street block. To avoid reducing the land use efficiency, the plot ratio in these two cases were same. The site coverage ratios (λ_p) in Case 1 and 2 were respectively 0.51 and 0.42. The averaged building permeability (P) of the total area was estimated at 0–60 m above the ground and was 0.7 in Case 1 and 0.5 in Case 2.

For comparison purpose, a CFD simulation study was conducted to model air flows and traffic air pollutant dispersion in the above two cases. The simulations were constructed in accordance with the methodology in the parametric study. The comparing results in

Fig. 14 demonstrated that the wind permeability in the entire area significantly increased in Case 2. Therefore, Case 2 significantly increased the local dispersion. The normalized concentration data was collected at the target street, and cross-compared in Fig. 15. It is clear that the probability of high concentration ($\bar{c} > 1.0$) in Case 2 was far much less than the one in Case 1. This result demonstrated the effectiveness of the suggested mitigation measures outlined in this study.

Based on the understanding in Section 4.4, the urban permeability λ_i was also calculated, which was 0.48 in Case 1 and 0.27 in Case 2. Similarly, the spatially averaged normalized concentration (\bar{c}) decreased from 0.79 in Case 1 to 0.59 in Case 2. These results coincided well with the linear relationship shown in Fig. 13 and validated that the understanding of urban permeability presented in Section 4.4 is feasible in the practical urban design.

6. Conclusion

In this study, a CFD parametric approach was taken to investigate the impact of urban permeability and building geometries on air pollutant dispersion in the high-density urban areas. The analysis and discussion of the results of this study revealed the following scientific understandings for the decision-making in high-density urban planning and design activities:

- 1) The SST $\kappa-\omega$ model can simulate the species transport in a street canyon with high accuracy and can be considered as a good design tool in urban planning and architecture design for air pollutant problems, due to the low computational cost. The performances of various modeling methods (LES and RANS) that are provided by ANSYS Fluent were investigated by cross-comparing with wind tunnel experiment results. Although LES is clearly more accurate than the RANS, the accuracy of the RANS model is sufficient to test the effects of planning and design activities on air pollutant concentration. Among the RANS models, the SST $\kappa-\omega$ model had the best performance because of the special near-wall region treatment using the standard $\kappa-\omega$ model.

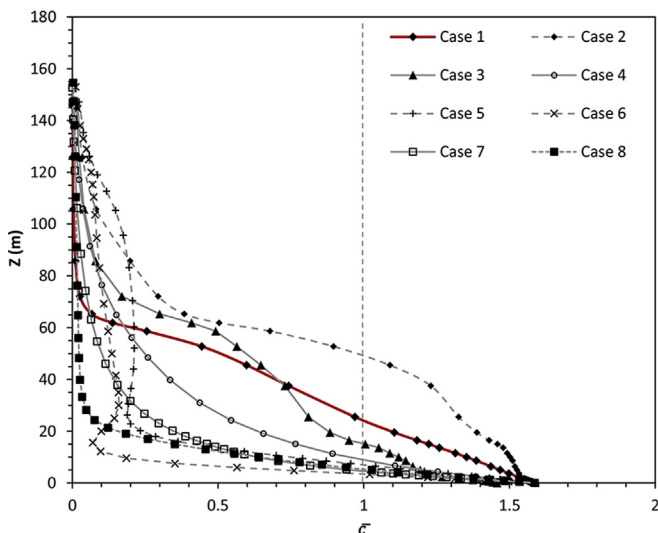


Fig. 10. Cross comparison of the vertical distributions of normalized concentration (\bar{c}) in Cases 1–8.

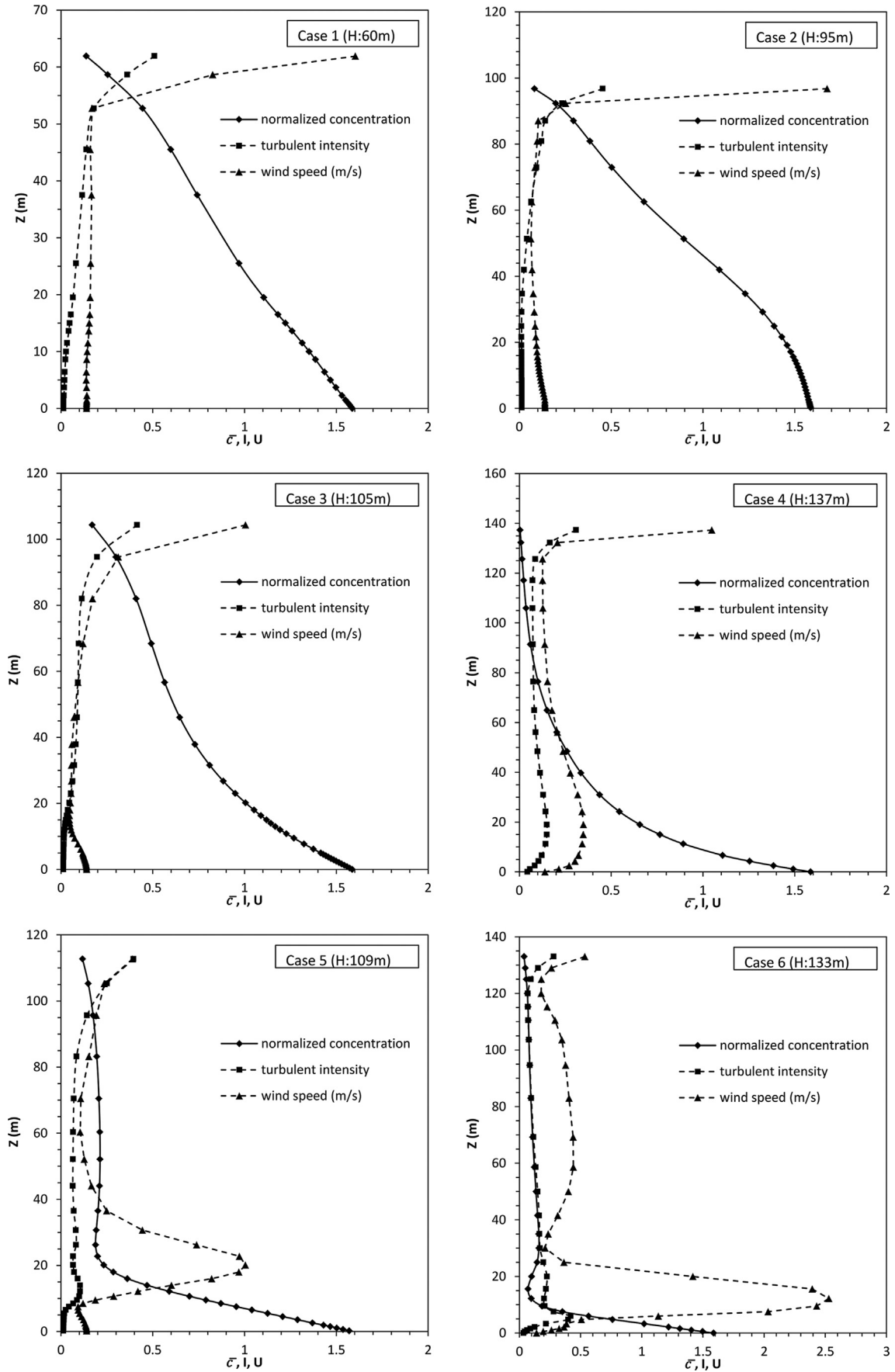


Fig. 11. Vertical profiles of normalized concentration (\bar{c}), turbulent intensity (I), and wind speed (U) in Cases 1–6. Building heights (H) in six cases are given.

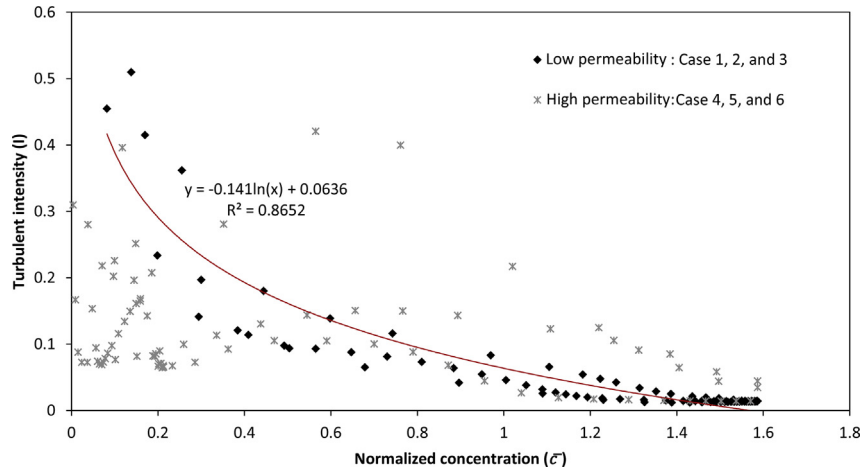


Fig. 12. Regression analysis of the relationship between turbulent intensity and normalized concentration in the street canyon at different cases with low and high permeability. (Significant level: 95%).

- 2) The simulation results validated that mitigation strategies for the air pollutant dispersion are necessary in the planning and design of high-density urban areas. In current urban conditions, traffic air pollutants are seriously concentrated in the deep street canyon. If current planning and design activities do not change, these conditions will worsen with future urban development. Given the negative effects of air pollution on public health and that of the high population density in Hong Kong, mitigation strategies are necessary to alleviate this impact.
- 3) The impacts of various urban planning and design strategies to improve air quality in both street canyons for pedestrian and inside adjacent buildings were quantitatively investigated and cross-compared in parametric studies. Policy makers can determine what needs to be changed by having a better understanding of how to select appropriate mitigation strategies in particular planning and design cases to mitigate the negative effects of air pollutant on the surrounding environments. Strategies recommended in this study can be applied into both the new project design and the urban redevelopment. The advantage of this kind of building-scale strategies is that they allow the urban redevelopment to be done step by step, one building by one building. It is more practical than the redevelopment done in one time.

This study noted that the air pollutant dispersion in high-density cities can occur if strategies which promote convection effects, such as building separation, porosity, and stepped podium void, are implemented and could be more efficient than strategies for larger turbulence diffusion, such as building setback. Unlike what the AVA understanding indicates, pedestrian-level pollutant concentration depends on the permeability of the entire street canyon. Although a high building porosity off ground level cannot increase the wind speed at pedestrian level, it can decrease pedestrian-level air pollutant concentrations. In the design and planning process, appropriate strategies need to be chosen based on the particular concerns in different projects.

- 4) Simulation results indicated that both the prevailing wind direction and urban permeability are important to estimate the direction of pedestrian level pollutant dispersion in high-density cities. Low urban permeability in high-density urban areas could reverse air flow near the ground, allowing air pollutants to disperse into the windward area of the pollutant sources.
- 5) By integrating the horizontal and vertical permeability based on Counihan's surface roughness model, a new permeability index λ_i was introduced to estimate the spatially averaged \bar{c} at the pedestrian area. The efficiency of this index was validated by a

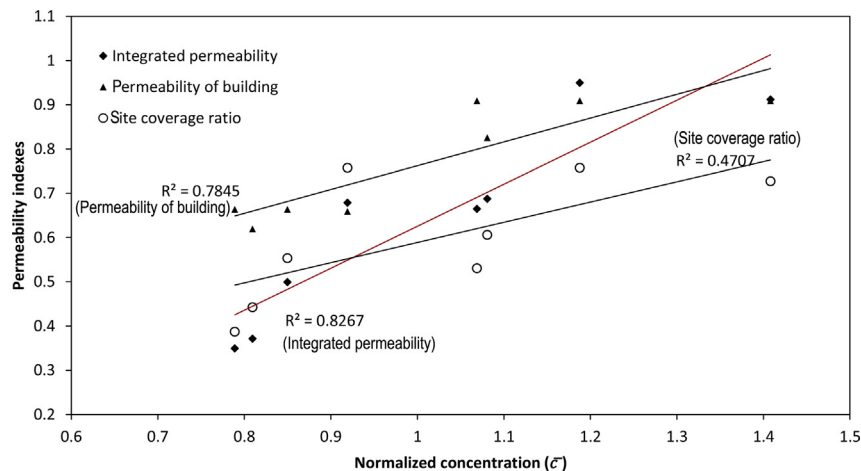


Fig. 13. Linear relationships between pedestrian level air pollutant concentration and permeability indexes, P , λ_p , and λ_i . (Significant level: 95%).

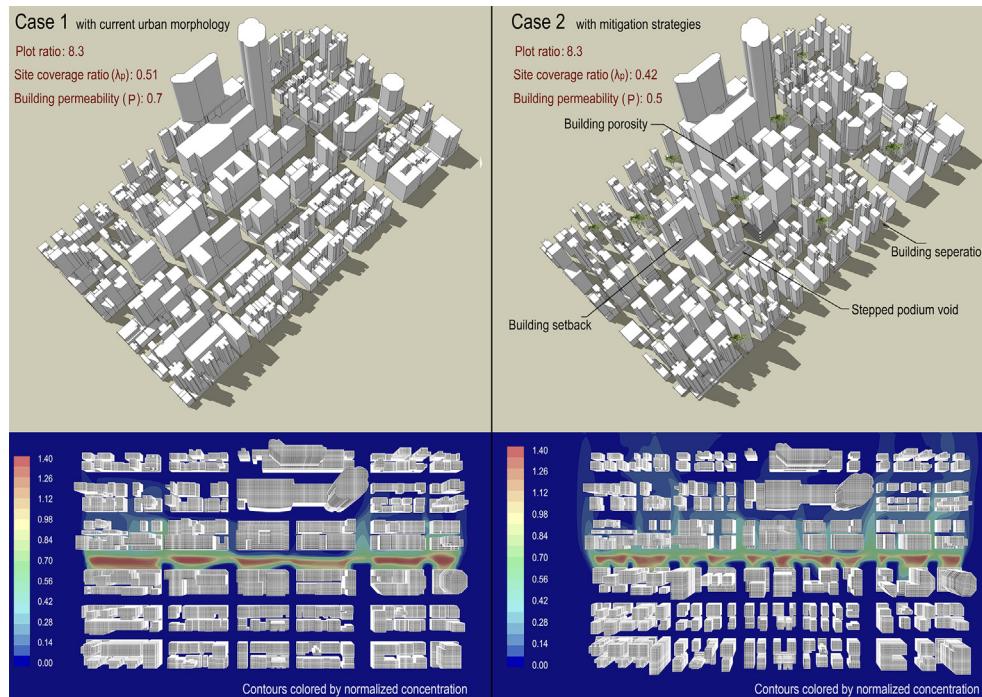


Fig. 14. Case study of urban redevelopment at Mong Kok and simulation results. Case 1: the current urban area of Mong Kok; Case 2: the urban morphology of Mong Kok with mitigation strategies. The mitigation strategies in Case 2 can significantly increase the wind permeability and decrease the traffic air pollutant concentration.

linear regression analysis. This result provided a possibility for mapping air quality in the urban areas with traffic volume data by using GIS technology.

7. Limitations and future study

It is considered that the convection is effective when pollutant sources are limited to areas and not uniformly presented in all streets, with the assumption that the concentration in neighboring street is lower than in the street with heavy traffic-related pollutant source. Therefore, modeling reactive pollutants is expected to be

included in future studies to extend the research to larger spatial and time scales to clarify the potential negative effects of diluted pollutant on the neighboring areas. Accordingly, field measurement or wind tunnel studies are necessary to validate the chemical reaction modeling. On the other hand, this study is the first stage of research on a planning and design guideline for urban air quality. Further parametric and real urban studies are necessary to determine threshold values of various design parameters and clarify the relationship between urban permeability and air pollutant dispersion.

Acknowledgment

The study is supported by the Post Graduate Scholarship (PGS) grant and the Global Scholarship Programme for Research Excellence-CNOOC Grant from The Chinese University of Hong Kong. Thanks are due to Professor Jimmy Fung of Hong Kong Science and Technology University for providing the MM5/CALMET data. The authors also wish to give special thanks to the referees for their valuable comments which help to improve the paper.

References

- [1] World Health Organization. Air quality and health – fact sheet No 313. <http://www.who.int/mediacentre/factsheets/fs313/en/2008>.
- [2] European Environment Agency. Air quality in Europe – 2012 report; 2012. Copenhagen, Denmark.
- [3] Kunzli N, Kaiser R, Medina S, Studnicka M, Chanel O, Filliger P, et al. Public-health impact of outdoor and traffic-related air pollution: a European assessment. *Lancet* 2000;356:795–801.
- [4] Environmental Protection Department. Air quality in Hong Kong 2011 – a report on the results from the air quality monitoring network (AQMN). Hong Kong: The Government of the Hong Kong Special Administrative Region; 2011.
- [5] Grice S, Stedman J, Kent A, Hobson M, Norris J, Abbott J, et al. Recent trends and projections of primary NO₂ emissions in Europe. *Atmos Environ* 2009;43:2154–67.
- [6] Ng E, Yuan C, Chen L, Ren C, Fung JCH. Improving the wind environment in high-density cities by understanding urban morphology and surface roughness: a study in Hong Kong. *Landscape Urban Plann* 2011;101:59–74.

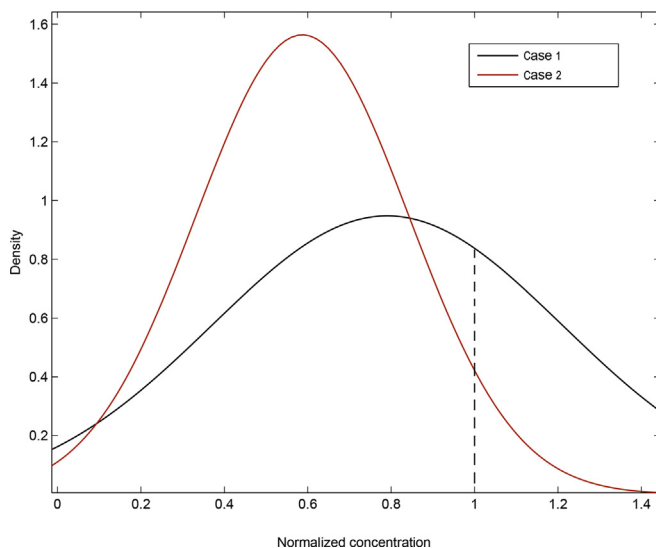


Fig. 15. Distribution of the normalized concentrations in Case 1 and Case 2. The probability of high concentration ($\bar{c} > 1.0$) in Case 2 is far much less than the one in Case 1.

- [7] Yim SHL, Fung JCH, Lau AKH, Kot SC. Air ventilation impacts of the “wall effect” resulting from the alignment of high-rise buildings. *Atmos Environ* 2009;43:4982–94.
- [8] Hang J, Li YG, Sandberg M, Buccolieri R, Di Sabatino S. The influence of building height variability on pollutant dispersion and pedestrian ventilation in idealized high-rise urban areas. *Build Environ* 2012;56:346–60.
- [9] Tominaga Y, Stathopoulos T. CFD modeling of pollution dispersion in building array: evaluation of turbulent scalar flux modeling in RANS model using LES results. *J Wind Eng Ind Aerod* 2012;104:484–91.
- [10] Li XX, Liu CH, Leung DYC, Lam KM. Recent progress in CFD modelling of wind field and pollutant transport in street canyons. *Atmos Environ* 2006;40:5640–58.
- [11] Kristensson A, Johansson C, Westerholm R, Swietlicki E, Gidhagen L, Wideqvist U, et al. Real-world traffic emission factors of gases and particles measured in a road tunnel in Stockholm, Sweden. *Atmos Environ* 2004;38:657–73.
- [12] Ho KF, Ho SSH, Lee SC, Cheng Y, Chow JC, Watson JG, et al. Emissions of gas-and particle-phase polycyclic aromatic hydrocarbons (PAHs) in the Shing Mun Tunnel, Hong Kong. *Atmos Environ* 2009;43:6343–51.
- [13] Baik JJ, Kang YS, Kim JJ. Modeling reactive pollutant dispersion in an urban street canyon. *Atmos Environ* 2007;41:934–49.
- [14] Kikumoto H, Ooka R. A numerical study of air pollutant dispersion with bimolecular chemical reactions in an urban street canyon using large-eddy simulation. *Atmos Environ* 2012;54:456–64.
- [15] Salim SM, Buccolieri R, Chan A, Di Sabatino S. Numerical simulation of atmospheric pollutant dispersion in an urban street canyon: comparison between RANS and LES. *J Wind Eng Ind Aerod* 2011;99:103–13.
- [16] Tominaga Y, Stathopoulos T. CFD modeling of pollution dispersion in a street canyon: comparison between LES and RANS. *J Wind Eng Ind Aerod* 2011;99:340–8.
- [17] Gousseau P, Blocken B, Stathopoulos T, Van HeijstG JF. CFD simulation of near-field pollutant dispersion on a high-resolution grid: a case study by LES and RANS for a building group in downtown Montreal. *Atmos Environ* 2010;45:428–38.
- [18] Pontiggia M, Derudi M, Alba M, Scaioni M, Rota R. Hazardous gas releases in urban areas: assessment of consequences through CFD modelling. *J Hazard Mater* 2010;176:589–96.
- [19] Gousseau P, Blocken B, van Heijst GJF. CFD simulation of pollutant dispersion around isolated buildings: on the role of convective and turbulent mass fluxes in the prediction accuracy. *J Hazard Mater* 2011;194:422–34.
- [20] Huang H, Ooka R, Chen H, Kato S, Takahashi T, Watanabe T. CFD analysis on traffic-induced air pollutant dispersion under non-isothermal condition in a complex urban area in winter. *J Wind Eng Ind Aerod* 2008;96:1774–88.
- [21] Mirzaei PA, Haghighat F. A procedure to quantify the impact of mitigation techniques on the urban ventilation. *Build Environ* 2012;47:410–20.
- [22] Eeftens M, Beekhuizen J, Beelen R, Wang M, Vermeulen R, Brunekreef B, et al. Quantifying urban street configuration for improvements in air pollution models. *Atmos Environ* 2013;72:1–9.
- [23] Buccolieri R, Sandberg M, Di Sabatino S. City breathability and its link to pollutant concentration distribution within urban-like geometries. *Atmos Environ* 2010;44:1894–903.
- [24] Richmond-Bryant J, Reff A. Air pollution retention within a complex of urban street canyons: a two-city comparison. *Atmos Environ* 2012;49:24–32.
- [25] Ng E. Policies and Technical guidelines for urban planning of high density cities – air ventilation assessment (AVA) of Hong Kong. *Build Environ* 2009;44.
- [26] Hong Kong Building Department. Sustainable building design guidelines. Practical note for authorized persons, registered structure engineers and registered geotechnical engineers. Hong Kong: APP-152; 2006.
- [27] Yuan C, Ng E. Building porosity for better urban ventilation in high-density cities - a computational parametric study. *Build Environ* 2012;50:176–89.
- [28] Ng E. Towards a planning and practical understanding for the need of meteorological and climatic information for the design of high density cities – a case based study of Hong Kong. *Int J Climatology* 2012;32:582–98.
- [29] Murakami S. Environmental design of outdoor climate based on CFD. *Fluid Dyn Res* 2006;38:108–26.
- [30] Wang M, Lin CH, Chen QY. Advanced turbulence models for predicting particle transport in enclosed environments. *Build Environ* 2012;47:40–9.
- [31] Zhang Z, Chen Q. Experimental measurements and numerical simulations of particle transport and distribution in ventilated rooms. *Atmos Environ* 2006;40:3396–408.
- [32] Fluent Inc. FLUENT 14.0 theory guide; 2012.
- [33] Tominaga Y, Mochida A, Yoshie R, Kataoka H, Nozu T, Yoshikawa M, et al. AIJ guidelines for practical applications of CFD to pedestrian wind environment around buildings. *J Wind Eng Ind Aerod* 2008;96:1749–61.
- [34] Tominaga Y, Mochida A, Murakami S, Sawaki S. Comparison of various revised k-epsilon models and LES applied to flow around a high-rise building model with 1: 1: 2 shape placed within the surface boundary layer. *J Wind Eng Ind Aerod* 2008;96:389–411.
- [35] Menter FR, Kuntz M, Langtry R. Ten years of industrial experience with the SST turbulence model. *Turbul Heat Mass Trans* 2003;4:625–32.
- [36] Mochida A, Murakami S, Ojima T, Kim S, Ooka R, Sugiyama H. CFD analysis of mesoscale climate in the Greater Tokyo area. *J Wind Eng Ind Aerod* 1997;67:68:459–77.
- [37] Kondo H, Asahi K, Tomizuka T, Suzuki M. Numerical analysis of diffusion around a suspended expressway by a multi-scale CFD model. *Atmos Environ* 2006;40:2852–9.
- [38] Ashie Y, Hirano K, Kono T. Effects of sea breeze on thermal environment as a measure against Tokyo's urban heat island. Yokohama, Japan: The Seventh International Conference on Urban Climate; 2009.
- [39] Givoni B. Man, climate and architecture. New York: Elsevier; 1969.
- [40] Ng E, Wong NH, Han M. In: Bay JH, Ong BL, editors. Parametric studies of urban design morphologies and their implied environmental performance. London: Architectural Press; 2006.
- [41] Blocken B, Stathopoulos T, Carmeliet J. CFD simulation of the atmospheric boundary layer: wall function problems. *Atmos Environ* 2007;41:238–52.
- [42] Stathopoulos T, Storms R. Wind environmental conditions in passages between buildings. *Wind Eng Ind Aerodynamics* 1986;95:941–62.
- [43] Yim SHL, Fung JCH, Lau AKH. Mesoscale simulation of year-to-year variation of wind power potential over southern China. *Energies* 2009;2:340–61. <http://dx.doi.org/10.3390/en20200340>.
- [44] Vardoulakis S, Fisher BEA, Pericleous K, Gonzalez-Flesca N. Modelling air quality in street canyons: a review. *Atmos Environ* 2003;37:155–82.
- [45] Grimmond CSB, Oke TR. Aerodynamic properties of urban areas derived from analysis of surface form. *J Appl Meteorol* 1999;38:1262–92.